Shift-Variance of Linear Periodically Shift-Variant Systems and Non-stationarity of Wide-sense Cyclostationary Random Processes

Bashir Sadeghi

Submitted to the
Institute of Graduate Studies and Research
in partial fulfillment of the requirements for the degree of

Master of Science
in
Electrical and Electronic Engineering

Eastern Mediterranean University
September, 2013
Gazimagusa, North Cyprus

Approval of the Institute of Graduate Studies and Research

Prof. Dr. Elvan Yılmaz
Director

I certify that this thesis satisfies the requirements as a thesis for the degree of Master of Science in Electrical and Electronic Engineering.

Prof. Dr. Aykut Hocanın
Chair, Department of Electrical and Electronic Engineering

We certify that we have read this thesis and that in our opinion it is fully adequate in scope and quality as a thesis for the degree of Master of Science in Electrical and Electronic Engineering.

Prof. Dr. Runyi Yu
Supervisor

Examining Committee

1. Prof. Dr. Aykut Hocanın _____

2. Prof. Dr. Osman Kükrer _____

3. Prof. Dr. Runyi Yu _____

ABSTRACT

We study shift-variance of linear periodically shift-variant (LPSV) systems and non-stationarity of wide-sense cyclostationary (WSCS) random processes (with continuous-time input and output). We determine how far an LPSV system is away from the space of linear shift-invariant systems. We consider the average of commutator's norm as a shift-variance level, and the normalized version of it is then defined to be a shift-variance measure (SVM). Extending these ideas to random processes, we then consider non-stationarity of WSCS random processes based on the SVM of the autocorrelation operator of the process. We also introduce the expected shift-variance (which is a kind of SVM) for LPSV systems when the input is wide-sense stationary (WSS) random process, allowing us to investigate properties of output of an LPSV system when its input is a WSS random process. Finally, we analyze shift-variance and non-stationarity of generalized sampling-reconstruction processes, discrete wavelet transforms, double sideband amplitude modulated signals and double sideband amplitude modulation systems.

Keywords: Linear periodically shift-variant system, Shift-variance, Generalized sampling-reconstruction process, Non-stationarity

ÖZ

Bu çalışmada, doğrusal periyodik kayan-değişke sistemlerin (LPSV) kayma farkları ve geniş anlamda dönemli durağan (WSCS) rastgele süreçlerin (sürekli zaman giriş ve çıkış) durağan olmama durumu incelenmiştir. Bir LPSV sistemin doğrusal kayan-değismez sistem uzayından uzaklığı belirlenmiştir. Komütatör normunum ortalaması, bir kayma farkı düzeyi olarak ele alınmış ve normalize değerleri kayma farkı ölçüsü (SVM) olarak tanımlanmıştır. Bu düşünceler, rastgele süreçlere uygulanarak, geniş anlamda dönemli durağan (WSCS) rastgele süreçlerin durağan olmama durumu, sürecin oto-korelasyonunun kayma farkı ölçüsüne (SVM) uyarlanmıştır. Ayrıca, doğrusal periyodik kayan-değişke sistemlerin (LPSV) kayma farkı, giriş değişkeni geniş anlamda durağan (WSS) bir süreç iken açıklanmıştır. Bu durum, LPSV sistemin girişi geniş anlamda durağan iken, sistemin çıkışını incelememize olanak sağlar. Son olarak, genelleştirilmiş örnekleme yapılandırmasının, ayrık dalgacık dönüşümünün, çift yan bant genlik modülasyonlu işaretlerin ve çift yan bant genlik modülasyon sistemlerinin kayma farkı ve durağan olmaması incelenmiştir.

Anahtar Kelimeler: Doğrusal Periyodik Kayan-Değişke Sistem, Kayma Farkı, Genelleştirilmiş Örnekleme Yapılandırması Süreci, Durağan Olmama

This thesis is dedicated to

the memory of my beloved father, my first and greatest teacher;

my loving mother, who always supports and encourages me; and

my dear sister and brother, for their kindness and supports.

ACKNOWLEDGMENTS

I am deeply grateful to my supervisor Prof. Dr. Runyi Yu for his guidance and supervision, without which this research would not have been possible. I very much appreciate him for all he has done for me. I would also like to thank the committee members for their suggestions in finalizing the thesis. Special thanks go to Prof. Dr. Aykut Hocanın for his kind help in my understanding of probability and random processes.

TABLE OF CONTENTS

LIST OF FIGURES

LIST OF TABLES

LIST OF SYMBOLS / ABBREVIATIONS

G	Linear Shift-Invariant System
H	Linear System
K	Commutator System
T	Period and Sampling Time
$\overline{x}$	Complex conjugation of x
ω_c	Carrier Radian frequency
τ	Shift Operator
DCS	Degree of Cyclostationarity
DSB-AM	Double Sideband Amplitude Modulation
ESV	Expected Shift-Variance
LSI	Linear Shift-Invariant
NSt	Non-Stationarity
SVL	Shift-Variance Level
SVM	Shift-Variance Measure
$T-$LPSV	Linear Periodically Shift-Variant with period T
WSCS	Wide-Sense Cyclostationary
WSS	Wide-Sense Stationary

Chapter 1

INTRODUCTION

Many physical systems are linear periodically shit-variant (LPSV). Example includes sampling-reconstruction processes, multirate filter banks, gating operators with periodic gate (amplitude modulation (AM) with sinusoidal carrier) and discrete wavelet transforms (DWTs).

Many random processes are wide-sense cyclostationary (WSCS). In telecommunications, signal processing, radar, sonar and telemetry applications, cyclostationarity is due to reconstruction process, modulation, coding, multiplexing. In mechanics it is coming from, for example, vibration of moving parts. In econometrics, cyclostationarity results from seasonality; and in atmospheric science it is caused by rotation and revolution of the earth [9].

Shift-variance and non-stationarity are two important issues in the study of linear shift-variant systems and random processes. They have found applications in many fields, including communications and signal processing, see [4] and [9].

Recently, Aach and Führ studied shift-variance properties of multirate filterbanks with either deterministic or random inputs [4]. They analyzed shift-variance of the filterbank and calculated the non-stationarity of its cyclostationary output. For generalized sampling processes, Yu performed shift-variance analysis in the deterministic setting [21]. In this thesis, we report our extension of the results to

linear periodically shift-variant (LPSV) systems whose inputs and outputs are both of continuous-time.

As in [4], we also consider the effect of LPSV systems on the deterministic and random signals. We apply an inner product and consequently the induced norm in Hilbert space of linear systems. We define the average of commutator's norm as shift-variance level (SVL). The normalized version of it is defined to be the shift-variance measure (SVM). We show that the SVL is equivalent to the distance between the LPSV system and the space of linear shift-invariant (LSI) systems. To study non-stationarity of cyclostationary random processes, we follow the idea of [4] and [22] to link the non-stationarity to the shift-variance of the associated autocorrelation operator (or function). This is because a random process is wide-sense stationary (WSS) if and only if (iff) the autocorrelation operator is shift-invariant; and it is wide-sense cyclostationary (WSCS) iff the operator is LPSV. We then obtain a kind of non-stationarity based on the SVM of the autocorrelation operator. This non-stationarity also characterizes the normalized distance from the autocorrelation of a random process to the autocorrelation of a nearest WSS process. Following [4], we also consider a particular SVM for LPSV systems (expected shift-variance) when the input is WSS random process.

Finally as particular applications, we treat generalized sampling-reconstruction processes, discrete wavelet transforms (DWTs) and double sideband amplitude modulated (DSB-AM) signal and double sideband amplitude modulation (DSB-AM) systems. For the sake of minimum error reconstruction, we assume that the sampling and reconstruction kernels form Riesz biorthogonal basis [18]. The SVM, the expected shift-variance of sampling-reconstruction process (which is an LPSV

system), and the non-stationarity of the output signal are then determined. Illustrative examples are provided.

The main results of this thesis has been reported in our paper [14].

1.1 Outline

The thesis consists of five chapters. In chapter 2 we talk about linear systems, particulary about LSI and LPSV systems. We then define a norm of LPSV systems and we use it to define SVL and SVM of LPSV systems. In chapter 3 after briefly talking about WSS and WSCS random processes, we define non-stationarity of WSCS random processes by bridging it to the SVM of LPSV systems. Also we define expected shift-variance measure for LPSV systems with the input being WSS random processes. Chapter 4 is about three applications: generalized sampling-reconstruction processes, DWTs, DSB-AM signals and systems. In chapter 5 we conclude the thesis and talk about future work.

Chapter 2

SHIFT-VARIANCE ANALYSIS OF LPSV SYSTEMS

We start this chapter with some basic definitions. The main aim is to determine the nearest shift-invariant system and the shift-variance measure for LPSV systems.

2.1 Introduction

Let L^2 be the Hilbert space of square integrable continuous-time functions and $H\,(L^2 \to L^2)\colon x(t) \mapsto y(t)$ be a bounded linear system. Denote by $\mathcal{B}$ the space of all bounded linear systems. For every $H \in \mathcal{B}$, we can specify it completely by the time domain input-output relation as

$$y(t) = [Hx](t) = \int_{-\infty}^{\infty} k(t,s)\,x(s)\,\mathrm{ds} = \int_{-\infty}^{\infty} h(t,s)\,x(t-s)\,\mathrm{ds} \tag{2.1}$$

where $k(t,s)$ and $h(t,s)$ are called Green's function and impulse response respectively [5]. Note that $k(t,s)$ is response of H to the shifted impulse function $\delta_s(\cdot) = \delta(\cdot - s)$, thus $[H\delta_s](t) = k(t,s) = h(t,t-s)$ and $h(t,s) = k(t,t-s)$.

Consider $\mathcal{B}_0$ the subspace of all bounded linear shift-invariant (LSI) systems which is denoted by. If $H \in \mathcal{B}_0$, we have $y(\cdot - t_0) = Hx(\cdot - t_0)$ for all $t_0 \in \mathbb{R}$, $x \in L^2$. Consequently from equation (2.1) we get

$$\int_{-\infty}^{\infty} h(t-t_0,s)x(t-t_0-s)\,\mathrm{ds} = \int_{-\infty}^{\infty} h(t,s)x(t-t_0-s)\,\mathrm{ds} \quad \text{for all } t_0\,, t \in \mathbb{R}\,, x \in L^2$$

That means $h(t-t_0,s) = h(t,s)$ for all $t_0\,, s\,, t \in \mathbb{R}$. Clearly now $h(t,s)$ independent of

t. Thus without any ambiguity, we can write $h(t,s) = h(s)$ or equivalently $k(t,s) = h(t-s)$. In this situation the time domain input-output relation becomes

$$y(t) = \int_{-\infty}^{\infty} h(s)\, x(t-s)\, \mathrm{ds} = [h * x](t) \tag{2.2}$$

where $*$ is the convolution operator.

For each $T > 0$, denoted by $\mathcal{B}_T$ the subspace of all bounded linear shift-variant systems satisfying $y(\cdot + T) = Hx(\cdot + T)$ for any $x \in L^2$. Systems in $\mathcal{B}_T$ are also referred to as linear periodically shift-variant (LPSV) systems [4] (with period of T). It can be shown that the impulse response is $T-$periodic as a function of t, thus we have

$$h(t-T,s) = h(t,s) \tag{2.3}$$

Throughout this thesis, we assume that $H \in \mathcal{B}_T$ and note that $\mathcal{B}_0 \subset \mathcal{B}_T$. Since $h(t,s)$ is periodic in t with period T, we can express the impulse response as Fourier series:

$$h(t,s) = \sum_{k\in\mathbb{Z}} h_k(s)\, e^{jk\omega_0 t} \tag{2.4}$$

where $\omega_0 = 2\pi/T$ and $\mathbb{Z}$ is the set of integer numbers. The coefficients are

$$h_k(s) = \frac{1}{T} \int_{-T/2}^{T/2} h(t,s)\, e^{-jk\omega_0 t}\, \mathrm{dt} \tag{2.5}$$

Let $\hat{h}(t,\xi)$ be the Fourier transform of $h(t,s)$ with respect to s ($\hat{x}$ indicates the Fourier transform of x). As a function of t, $\hat{h}(t,\xi)$ is also periodic in t with period of T. Thus we can represent $\hat{h}(t,\xi)$ (as a function of t) as Fourier series:

$$\hat{h}(t,\xi) = \sum_{k\in\mathbb{Z}} \hat{h}_k(\xi)\, e^{jk\omega_0 t} \tag{2.6}$$

where

$$\hat{h}_k(\xi) = \frac{1}{T}\int_{-T/2}^{T/2} \hat{h}(t,\xi)\, e^{-jk\omega_0 t}\,\mathrm{dt} \tag{2.7}$$

Note that $\hat{h}_k(\xi)$ is actually the Fourier transform of $h_k(s)$. As we shall see in the next section, the Fourier series decomposition gives more insights to analyze the LPSV systems.

2.2 Norm of LPSV Systems

Let us define the inner product between systems H_1 and H_2 in the space of $\mathcal{B}_T$ as

$$\begin{aligned} \langle H_1, H_2 \rangle &= \frac{1}{T}\int_{-T/2}^{T/2} \langle H_1\delta_s(\cdot), H_2\delta_s(\cdot)\rangle\,\mathrm{ds} \\ &= \frac{1}{T}\int_{-T/2}^{T/2}\int_{-\infty}^{\infty} h_1(t,t-s)\,\overline{h_2(t,t-s)}\,\mathrm{dt}\,\mathrm{ds} \end{aligned} \tag{2.8}$$

where h_1 and h_2 are the corresponding impulse responses and over bar denotes complex conjugation. By change of variable $u = t - s$, we get

$$\langle H_1, H_2 \rangle = \frac{1}{T}\int_{-T/2}^{T/2}\int_{-\infty}^{\infty} h_1(s+u,u)\,\overline{h_2(s+u,u)}\,\mathrm{du}\,\mathrm{ds}$$

Since the integration of periodic functions is the same over each period, we have

$$\langle H_1, H_2 \rangle = \frac{1}{T}\int_{-T/2}^{T/2}\int_{-\infty}^{\infty} h_1(s,u)\,\overline{h_2(s,u)}\,\mathrm{du}\,\mathrm{ds} \tag{2.9}$$

Now, the induced norm (squared) of H by the inner product is

$$\|H\|^2 = \langle H, H\rangle = \frac{1}{T}\int_{-T/2}^{T/2}\int_{-\infty}^{\infty} |h(t,s)|^2\,\mathrm{ds}\,\mathrm{dt} \tag{2.10}$$

By using Parseval's relations for Fourier series and Fourier transforms, we can express the norm in the Fourier domain as

$$\begin{aligned} \|H\|^2 &= \sum_{k\in\mathbb{Z}} \int_{-\infty}^{\infty} |h_k(s)|^2 \,\mathrm{d}s \\ &= \frac{1}{2\pi} \sum_{k\in\mathbb{Z}} \int_{-\infty}^{\infty} |\hat{h}_k(\xi)|^2 \,\mathrm{d}\xi \end{aligned} \tag{2.11}$$

Let $G \in \mathcal{B}_0$ and g be its impulse response (i.e., $g(s) = [G\delta](s)$). The distance (squared) between H and G can be defined as

$$\begin{aligned} d^2(H,G) &= \|H-G\|^2 \\ &= \frac{1}{T} \int_{-T/2}^{T/2} \int_{-\infty}^{\infty} |h(t,s) - g(s)|^2 \,\mathrm{d}s\,\mathrm{d}t \end{aligned} \tag{2.12}$$

And using Parseval's relation for Fourier series, gives us

$$d^2(H,G) = \int_{-\infty}^{\infty} (|h_0(s) - g(s)|^2 + \sum_{k\neq 0} |h_k(s)|^2) \,\mathrm{d}s \tag{2.13}$$

The above expression allows us to determine the closest LSI system (denoted by) G_c. It is specified by the impulse response as

$$g_c(s) = h_0(s) = \frac{1}{T} \int_{-T/2}^{T/2} h(t,s) \,\mathrm{d}t \tag{2.14}$$

Note that G_c is the orthogonal projection of H onto the subspace $\mathcal{B}_0$ and the impulse response $g_c(s)$ is the DC component of $h(t,s)$ as a function of t. We now have the distance (squared) between H and $\mathcal{B}_0$ as

$$d^2(H,\mathcal{B}_0) = \frac{1}{T} \int_{-T/2}^{T/2} \int_{-\infty}^{\infty} |h(t,s) - g_c(s)|^2 \,\mathrm{d}s \tag{2.15}$$

That is,

$$d^2(H,\mathcal{B}_0) = \sum_{k\neq 0}\int_{-\infty}^{\infty} |h_k(s)|^2 \mathrm{ds} \tag{2.16}$$

And in the frequency domain it becomes

$$d^2(H,\mathcal{B}_0) = \frac{1}{2\pi}\sum_{k\neq 0}\int_{-\infty}^{\infty} |\hat{h}_k(\xi)|^2 \,\mathrm{d}\xi \tag{2.17}$$

2.3 Shift-Variance Level and Shift-Variance Measure for LPSV Systems

Let $\tau_{t_0}: x(t) \mapsto x(t-t_0)$ be the shift operator. If system $H \in \mathcal{B}_0$, the output $H\tau_{t_0}x$ is equal to $\tau_{t_0}Hx$ for all $x \in L^2$ and $t_0 \in \mathbb{R}$. When system H is not LSI, the difference signal $d = H\tau_{t_0}x - \tau_{t_0}Hx$ is not equal to zero for some input x and shift t_0. Similar to [2], for each t_0, we introduce below an error system (commutator system) which generates the difference signal:

$$\mathcal{K}_{t_0} = H\tau_{t_0} - \tau_{t_0}H \tag{2.18}$$

It can be shown that the impulse response of $\mathcal{K}_{t_0}$ is

$$\kappa_{t_0}(t,s) = h(t,s-t_0) - h(t-t_0,s-t_0) \tag{2.19}$$

Note that the commutator system is a T-LPSV system. As a result, its norm $\|\mathcal{K}_{t_0}\|$ is $T-$periodic as a function of t_0. Thus the shift variance level of H can then be defined

as

$$\mathrm{SVL}^2(H) = \frac{1}{T}\int_{-T/2}^{T/2} \|\mathcal{K}_{t_0}\|^2 \,\mathrm{d}t_0 \tag{2.20}$$

which is the average value of the commutator's norm along all shift t_0 in one period. Intuitively, the shift-variance level and the distance to the nearest LSI system should be related. This is indeed the case as given in the following result.

Theorem 1 *The shift-variance level of H and its distance to $\mathcal{B}_0$ is related as*

$$\mathrm{SVL}(H) = \sqrt{2}\, d(H, \mathcal{B}_0) \tag{2.21}$$

The proof is given in Appendix A.

Since G_c is orthogonal projection of H onto $\mathcal{B}_0$, we obtain

$$\|H\|^2 = \|G_c\|^2 + d^2(H, \mathcal{B}_0) \tag{2.22}$$

Therefore there is an upper-bound for SVL, that is

$$\mathrm{SVL}(H) = \sqrt{2} d(H, \mathcal{B}_0) \leq \sqrt{2}\|H\| \tag{2.23}$$

Following the idea in [20] and the above inequality motivates us to define a normalized shift-variance measure by dividing to the upper-bound:

$$\mathrm{SVM}(H) = \frac{\mathrm{SVL}(H)}{\sqrt{2}\,\|H\|} = \frac{d(H, \mathcal{B}_0)}{\|H\|} \tag{2.24}$$

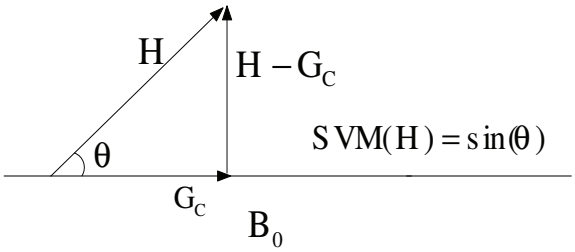

Figure 2.1: Geometrical Concept of SVM

Therefore

$$0 \leq \mathrm{SVM}(H) \leq 1 \tag{2.25}$$

We can represent the SVM (squared) as

$$\begin{aligned} \mathrm{SVM}^2(H) &= 1 - \frac{\|G_c\|^2}{\|H\|^2} \\ &= 1 - \frac{\int_{-\infty}^{\infty} |\hat{h}_0(\xi)|^2 \, \mathrm{d}\xi}{\sum_{k\in\mathbb{Z}} \int_{-\infty}^{\infty} |\hat{h}_k(\xi)|^2 \, \mathrm{d}\xi} \end{aligned} \tag{2.26}$$

Note that $\mathrm{SVM}(H) = 0$ iff $H \in \mathcal{B}_0$ and $\mathrm{SVM}(H) = 1$ (maximally shift-variant) iff its h_0 is equal to zero. The geometrical concept of SVM is illustrated in Figure 2.1.

Chapter 3

NON-STATIONARITY AND SHIFT-VARIANCE ANALYSIS OF LPSV SYSTEMS WITH RANDOM INPUT

In this chapter, we shall study the non-stationarity of random processes by the shift variance of a linear system that is determined by the autocorrelation function. We define a special shift-variance measure for LPSV systems when they are excited by WSS random processes.

3.1 Introduction

Let $z : \mathbb{R} \to \mathbb{C}$ be a zero-mean continuous-time random process with $\mathcal{E}\{|z(t)|^2\} < \infty$ for all $t \in \mathbb{R}$, where $\mathcal{E}$ denotes the expectation operator. The autocorrelation function of z is defined as $r_z(t,s) = \mathcal{E}\{z(t)\,\overline{z(t-s)}\}$. The random process z is called WSS if $r_z(t,s)$ is independent of time, t; it is WSCS with period T (T-WSCS) if $r_z(t+T,s) = r_z(t,s)$. The concepts and notions for discrete-time random processes are similarly defined.

3.2 Non-stationarity of WSCS Random Processes

We consider the autocorrelation operator R_z as a deterministic linear system whose impulse response is specified as $R_z\delta_s = r_z(\cdot, \cdot - s)$. Note that z is WSS iff R_z is an LSI system and z is T-WSCS iff R_z is a T-LPSV system. This suggests that we can define non-stationarity (NSt) of $T-$WSCS random process z by shift-variance measure of linear system R_z:

$$\mathrm{NSt}(z) = \mathrm{SVM}(R_z) \tag{3.1}$$

and the impulse response of the closest LSI system R_c is found to be

$$r_c(s) = \frac{1}{T}\int_{-T/2}^{T/2} r_z(t,s)\,\mathrm{dt} \tag{3.2}$$

We point out that the degree of cyclostationarity (DCS) of z defined in [22] is related to $\mathrm{NSt}(z)$ as follows:

$$\mathrm{DCS}(z) = \frac{\|R_z\|\,\mathrm{NSt}(z)}{\|R_c\|} \tag{3.3}$$

Passing a WSS random process through an T-LPSV system H, generally introduces a T-WSCS random process. The autocorrelation function of output y which is denoted by $r_y(t,s)$ is

$$r_y(t,s) = \sum_{k\in\mathbb{Z}} r_k(s)\, e^{jk\omega_0 t} \tag{3.4}$$

where the coefficients are

$$r_k(s) = \sum_{l\in\mathbb{Z}} [h_{(k+l)} * r_x * \tilde{h}_l](s)\, e^{jl\omega_0 s} \tag{3.5}$$

and $\widetilde{h(\cdot)} = \overline{h(-\cdot)}$. In the Fourier domain, we have

$$S_k(\xi) = \sum_{l\in\mathbb{Z}} \hat{h}_{(k+l)}(\xi - l\omega_0) S_x(\xi - l\omega_0)\overline{\hat{h}_l(\xi - l\omega_0)} \tag{3.6}$$

where $S_x(\xi)$ is the power spectral density of x (i.e., the Fourier transform of r_x [13]). The proof is given in Appendix B. The non-stationarity generated by WSS random

process x when it passes through H is

$$\mathrm{NSt}^2(y) = 1 - \frac{\int_{-\infty}^{\infty} |\sum_{l\in\mathbb{Z}} [h_l * r_x * \tilde{h}_l](s)\, e^{jl\omega_0 s}|^2 \,\mathrm{ds}}{\sum_{k\in\mathbb{Z}} \int_{-\infty}^{\infty} |\sum_{l\in\mathbb{Z}} [h_{l+k} * r_x * \tilde{h}_l](s)\, e^{jl\omega_0 s}|^2 \,\mathrm{ds}} \tag{3.7}$$

And in the Fourier domain it becomes

$$\mathrm{NSt}^2(y) = 1 - \frac{\int_{-\infty}^{\infty} |\sum_{l\in\mathbb{Z}} |\hat{h}_l(\xi - l\omega_0)|^2 S_x(\xi - l\omega_0)|^2 \,\mathrm{d}\xi}{\sum_{k\in\mathbb{Z}} \int_{-\infty}^{\infty} |\sum_{l\in\mathbb{Z}} \hat{h}_{k+l}(\xi - l\omega_0) S_x(\xi - l\omega_0) \overline{\hat{h}_l(\xi - l\omega_0)}|^2 \,\mathrm{d}\xi} \tag{3.8}$$

Note that y is WSS if $\mathrm{NSt}(y) = 0$ and we see that for some particular LPSV systems under WSS input, output y can be WSS. This is the case when there is no intersection between the supports of $\hat{h}_n$ and $\hat{h}_m$ for $n \neq m$. In this situation, the denominator of fractional part in (3.8) is equal to the numerator of it, and therefore the $\mathrm{NSt}(y)$ becomes zero.

3.3 Expected Shift-Variance of LPSV Systems

Now assume that the input is random (for example a WSS process), how can we quantify the shift-variance of an LPSV system by considering the randomness of input? This problem was considered by Aach and Führ for multirate discrete-time systems [4]. They introduced the notation of expected shift-variance. Here we follow their idea and define the normalized version of expected shift-variance in [4] as expected shift-variance.

The output of commutator for WSS random process input x is

$$d_{t_0} = \mathcal{K}_{t_0} x = (H\tau_{t_0} - \tau_{t_0} H)\, x \tag{3.9}$$

If H is LSI, d_{t_0} is equal to zero for all shift t_0 and all input x. Now let H be a T-LPSV system. Then d_{t_0} is a T-WSCS random process and consequently $\mathcal{E}\{|d_{t_0}(t)|^2\} =$

$r_{d_{t_0}}(t,0)$ is T-periodic in both t and t_0. To quantify the shift-variance of H under a WSS input signal, we shall consider $\mathcal{E}\{|d_{t_0}(t)|^2\}$ over one period T, for both t and t_0. Similar to Aach and Führ [4] the first suggestion for expected shift-variance is

$$\sqrt{\frac{1}{T^2}\int_{-T/2}^{T/2}\int_{-T/2}^{T/2}\mathcal{E}\{|d_{t_0}(t)|^2\}\,\mathrm{d}t_0\,\mathrm{d}t} \tag{3.10}$$

However this measure is not normalized (it depends on the norm of H). In appendix C we obtain

$$\frac{\frac{1}{T^2}\int_{-T/2}^{T/2}\int_{-T/2}^{T/2}\mathcal{E}\{|d_{t_0}(t)|^2\}\,\mathrm{d}t_0\,\mathrm{d}t}{2(\frac{1}{T}\int_{-T/2}^{T/2}\mathcal{E}\{|y(t)|^2\}\,\mathrm{d}t)} = 1-\frac{\int_{-\infty}^{\infty}|\hat{h}_0(\xi)|^2 S_x(\xi)\,\mathrm{d}\xi}{\sum_{k\in\mathbb{Z}}\int_{-\infty}^{\infty}|\hat{h}_k(\xi)|^2 S_x(\xi)\,\mathrm{d}\xi} \leq 1 \tag{3.11}$$

Thus an upper-bound for the suggested expected shift-variance is

$$\sqrt{\frac{2}{T}\int_{-T/2}^{T/2}\mathcal{E}\{|y(t)|^2\}\,\mathrm{d}t} \tag{3.12}$$

Consequently a normalized expected shift-variance can be defined as

$$\begin{aligned}\mathrm{ESV}^2(H,x) &= \frac{\frac{1}{T^2}\int_{-T/2}^{T/2}\int_{-T/2}^{T/2}\mathcal{E}\{|d_{t_0}(t)|^2\}\,\mathrm{d}t_0\,\mathrm{d}t}{2(\frac{1}{T}\int_{-T/2}^{T/2}\mathcal{E}\{|y(t)|^2\}\,\mathrm{d}t)} \\ &= 1-\frac{\int_{-\infty}^{\infty}|\hat{h}_0(\xi)|^2 S_x(\xi)\,\mathrm{d}\xi}{\sum_{k\in\mathbb{Z}}\int_{-\infty}^{\infty}|\hat{h}_k(\xi)|^2 S_x(\xi)\,\mathrm{d}\xi}\end{aligned} \tag{3.13}$$

or in the time domain:

$$\mathrm{ESV}^2(H,x) = 1-\frac{\int_{-\infty}^{\infty}\int_{-\infty}^{\infty}h_0^*(t)\,h_0(t-s)r_x(s)\,\mathrm{d}s\,\mathrm{d}t}{\sum_{k\in\mathbb{Z}}\int_{-\infty}^{\infty}\int_{-\infty}^{\infty}h_k^*(t)\,h_k(t-s)r_x(s)\,\mathrm{d}s\,\mathrm{d}t} \tag{3.14}$$

From the above equation we can realize that ESV is equal to the SVM when the input is white noise (since $S_x(\xi)=1$). The ESV tells how different the expected value of the output for a shifted input from that of the shifted output. The ESV is zero iff H is LSI.

The Fourier domain expression (3.13) provides some insight as when an LPSV system would become LSI (see examples at Section 4.1).

Chapter 4

APPLICATIONS IN SIGNAL PROCESSING AND COMMUNICATIONS

4.1 Generalized Sampling-Reconstruction Processes

Sampling-reconstruction process plays an important role in signal processing and communications. In particular, the generalized sampling-reconstruction theory of Unser and Aldroubi [18] offers a versatile framework in studying many problems of sampling beyond Shannon.

In this section we investigate the non-stationarity and shift-variance of generalized sampling-reconstruction processes shown in Figure 4.1, where x is a zero-mean WSS random process; and for minimum error between input signal and the output signal (which is in the space of spanned by $\{\varphi(\cdot - nT)\}_n$), $\tilde{\varphi}(t)$ and $\varphi(t)$ are assumed to be dual (biorthogonal) Riesz basis [18], i.e., $\langle \varphi(\cdot - nT), \tilde{\varphi}(\cdot - mT) \rangle = \delta[n-m]$. In the Fourier domain they are related as [11]

$$\widehat{\tilde{\varphi}}(\xi) = \frac{T\hat{\varphi}(\xi)}{\sum_{n\in\mathbb{Z}} |\hat{\varphi}(\xi + n\omega_0)|^2} \tag{4.1}$$

We mention that sampling generally results in shift-variance whereas reconstruction introduces non-stationarity.

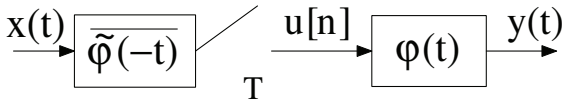

Figure 4.1: A Generalized Sampling and Reconstruction Process

Consider the sampling first. The output of sampling $u[n]$ is given by[1]

$$\begin{aligned} u[n] &= \langle x, \tilde{\varphi}(\cdot - nT)\rangle \\ &= \int_{-\infty}^{\infty} x(t)\,\overline{\tilde{\varphi}(t-nT)}\,\mathrm{dt} \end{aligned} \tag{4.2}$$

Here u is discrete-time and its Fourier transform is

$$\hat{u}(e^{j\xi T}) = \frac{1}{T}\sum_{n\in\mathbb{Z}} \overline{\hat{\tilde{\varphi}}(\xi + n\omega_0)}\,\hat{x}(\xi + n\omega_0) \tag{4.3}$$

The autocorrelation function of u is

$$\begin{aligned} r_u[n,k] &= \mathcal{E}\{u[n]\,\overline{u[n-k]}\} \\ &= \mathcal{E}\{\int_{-\infty}^{\infty} x(t_1)\,\overline{\tilde{\varphi}(t_1 - nT)}\,\mathrm{dt}_1 \int_{-\infty}^{\infty} \overline{x(t_2)}\,\tilde{\varphi}(t_2 - (n-k)T)\,\mathrm{dt}_2\} \end{aligned} \tag{4.4}$$

By change of variable $(t_1 + nT) \to t_1$ and $(t_2 + nT) \to t_2$ and using the WSS property of x we get

$$r_u[n,k] = \int_{-\infty}^{\infty}\int_{-\infty}^{\infty} \overline{\tilde{\varphi}(t_1)}\,\tilde{\varphi}(t_2 + kT)\,r_x(t_1 - t_2)\mathrm{dt}_1\,\mathrm{dt}_2 \tag{4.5}$$

Since r_u above is independent of n, thus u is a WSS discrete-time random process. The

[1]Note that the integration for random signals is in the mean square sense [10].

power spectral density of u is

$$S_u(e^{j\xi T}) = \frac{1}{T}\sum_{n\in\mathbb{Z}} |\widehat{\varphi}(\xi + n\omega_0)|^2 S_x(\xi + n\omega_0) \tag{4.6}$$

In the reconstruction part, the output is

$$y(t) = \sum_{n\in\mathbb{Z}} u[n]\,\varphi(t - nT) \tag{4.7}$$

Its Fourier transform is

$$\hat{y}(\xi) = \hat{u}(e^{j\xi T})\,\hat{\varphi}(\xi) \tag{4.8}$$

In view of the WSS property of u, the autocorrelation function of y becomes

$$\begin{aligned} r_y(t,s) = \mathcal{E}\{y(t)\overline{y(t-s)}\} &= \mathcal{E}\{\sum_{n_1\in\mathbb{Z}} u[n_1]\,\varphi(t-n_1T)\sum_{n_2\in\mathbb{Z}}\overline{u[n_2]\,\varphi(t-s-n_2T)}\} \\ &= \sum_{n_1\in\mathbb{Z}}\sum_{n_2\in\mathbb{Z}} \varphi(t-n_1T)\,\overline{\varphi(t-s-n_2T)}\,r_u[n_1-n_2] \end{aligned} \tag{4.9}$$

Now consider $r_y(t+T,s)$. By change of variable $(n_1+1)\to n_1$ and $(n_2+1)\to n_2$ we obtain $r_y(t+T,s) = r_y(t,s)$. Thus y is a T-WSCS random process. The relation between the Fourier transform of r_y and power spectral density of u is

$$(S_y)_k(\xi) = \frac{1}{T}\overline{\hat{\varphi}(\xi)}\hat{\varphi}(\xi + k\omega_0)S_u(e^{j\xi T}) \tag{4.10}$$

The proof is given in Appendix D.

Using (4.6) we obtain the relation between the Fourier transform of r_y and that the

power spectral density of x as

$$(S_y)_k(\xi) = \frac{1}{T^2}\overline{\hat{\varphi}(\xi)}\hat{\varphi}(\xi + k\omega_0)\sum_{n\in\mathbb{Z}}|\widehat{\tilde{\varphi}}(\xi + n\omega_0)|^2 S_x(\xi + n\omega_0) \tag{4.11}$$

where $S(t,\xi) = \sum_{k\in\mathbb{Z}}(S_y)_k(\xi)e^{jk\omega_0 t}$.

In order to analyze the shift-variance of system H in Figure 4.1, we need to determine its input-output relation. By direct substitution and change of variable, we obtain that

$$y(t) = Hx = \int_{-\infty}^{\infty} h(t,s)\,x(t-s)\,\mathrm{ds} \tag{4.12}$$

where

$$h(t,s) = \sum_{n\in Z}\overline{\tilde{\varphi}(t-s-nT)}\,\varphi(t-nT) \tag{4.13}$$

is the impulse response. By change of variable $(n-1)\to n$, we have $h(t+T,s) = h(t,s)$ (i.e., the generalized sampling-reconstruction process is an LPSV system). Following the procedure similar to that given in Appendix D, we obtain

$$\hat{h}_k(\xi) = \frac{1}{T}\overline{\widehat{\tilde{\varphi}}(\xi)}\,\hat{\varphi}(\xi + k\omega_0) \tag{4.14}$$

Note that since H in an LPSV system we could obtain equation (4.11) from (3.6) directly.

Using (4.1), we can obtain the impulse response as a function of only $\hat{\varphi}$ as

$$\hat{h}_k(\xi) = \frac{\overline{\hat{\varphi}(\xi)}\hat{\varphi}(\xi + k\omega_0)}{\sum_{n\in\mathbb{Z}}|\hat{\varphi}(\xi + n\omega_0)|^2} \tag{4.15}$$

Now we are ready apply the results in the previous chapters. First we obtain the norm of the sampling-reconstruction process as

$$\|H\|^2 = \frac{1}{2\pi}\sum_{k\in\mathbb{Z}}\int_{-\infty}^{\infty}|\hat{h}_k(\xi)|^2\,\mathrm{d}\xi = \frac{1}{2\pi}\int_{-\infty}^{\infty}\frac{|\hat{\varphi}(\xi)|^2}{\sum_{k\in\mathbb{Z}}|\hat{\varphi}(\xi+k\omega_0)|^2}\,\mathrm{d}\xi \tag{4.16}$$

and the norm of the closest LSI system is

$$\|G_c\|^2 = \frac{1}{2\pi}\int_{-\infty}^{\infty}|\hat{h}_0(\xi)|^2\,\mathrm{d}\xi = \frac{1}{2\pi}\int_{-\infty}^{\infty}\frac{|\hat{\varphi}(\xi)|^4}{\left(\sum_{k\in\mathbb{Z}}|\hat{\varphi}(\xi+k\omega_0)|^2\right)^2}\,\mathrm{d}\xi \tag{4.17}$$

Consequently the SVM of sampling-reconstruction process is

$$\mathrm{SVM}^2(H) = 1 - \frac{\int_{-\infty}^{\infty}\frac{|\hat{\varphi}(\xi)|^4}{(\sum_{k\in\mathbb{Z}}|\hat{\varphi}(\xi+k\omega_0)|^2)^2}\,\mathrm{d}\xi}{\int_{-\infty}^{\infty}\frac{|\hat{\varphi}(\xi)|^2}{\sum_{k\in\mathbb{Z}}|\hat{\varphi}(\xi+k\omega_0)|^2}\,\mathrm{d}\xi} \tag{4.18}$$

and the non-stationarity of output y is:

$$\mathrm{NSt}^2(y) = 1 - \frac{\int_{-\infty}^{\infty}|\hat{\varphi}(\xi)|^4 S_u^2(e^{j\xi T})\,\mathrm{d}\xi}{\int_{-\infty}^{\infty}|\hat{\varphi}(\xi)|^2\sum_{k\in\mathbb{Z}}|\hat{\varphi}(\xi+k\omega_0)|^2 S_u^2(e^{j\xi T})\,\mathrm{d}\xi} \tag{4.19}$$

Note that $S_u(e^{j\xi T})$ can be obtained from equation (4.6). From equation (4.19), it follows that if there is no intersection between the support of $\hat{\varphi}$ and u, then y is WSS. In this situation, the sampling-reconstruction process might not be LSI.

The expected shift-variance of sampling-reconstruction process under WSS input x is

$$\mathrm{ESV}^2(H,x) = 1 - \frac{\int_{-\infty}^{\infty}\frac{|\hat{\varphi}(\xi)|^4 S_x(\xi)}{(\sum_{k\in\mathbb{Z}}|\hat{\varphi}(\xi+k\omega_0)|^2)^2}\,\mathrm{d}\xi}{\int_{-\infty}^{\infty}\frac{|\hat{\varphi}(\xi)|^2 S_x(\xi)}{\sum_{k\in\mathbb{Z}}|\hat{\varphi}(\xi+k\omega_0)|^2}\,\mathrm{d}\xi} \tag{4.20}$$

If x is white noise then $S_x(\xi) = 1$, consequently $\mathrm{SVM}(H) = \mathrm{ESV}(H,x)$. In this case,

form (4.6) and (4.1) we have

$$S_u(e^{j\xi T}) = \frac{1}{T}\sum_{k\in\mathbb{Z}} |\widehat{\widetilde{\varphi}}(\xi + k\omega_0)|^2 = \frac{T}{\sum_{k\in\mathbb{Z}} |\hat{\varphi}(\xi + k\omega_0)|^2}$$

Substituting the above equality in equation (4.19) gives

$$\mathrm{SVM}(H) = \mathrm{ESV}(H,x) = \mathrm{NSt}(Hx) \tag{4.21}$$

In the following subsection, we consider two examples of sampling-reconstruction processes: we evaluate six different discrete wavelet transforms (DWTs) in the frame of sampling-reconstruction processes and we consider DSB-AM signals and systems. For input x we consider two examples:

1-White noise ($S_x(\xi) = 1$). In this case we have proved that the SVM, ESV, NSt are all the same. Thus we give only the value of SVM.

2-An autoregressive of order one (AR(1)) random process that is the response of the following LSI system to the input $w(t)$, :

$$\frac{\mathrm{d}}{\mathrm{dt}} x(t) + \alpha x(t) = w(t) \tag{4.22}$$

where $w(t)$ is white noise with $S_w(\xi) = 1$ and we take $\alpha = 0.9\pi$. Recall that $r_x(s) = 1/(2\alpha)\, e^{-\alpha|s|}$ and $S_x(\xi) = 1/(\xi^2 + \alpha^2)$ [10].

4.1.1 Shannon's Sampling

In the traditional Shannon's sampling, the kernel is $\varphi(t) = \frac{1}{T}\mathrm{sinc}(t/T)$. Thus we have $\hat{\varphi}(\xi) = \mathbf{1}_{[\frac{-\pi}{T},\frac{\pi}{T}]}(\xi)$, ($\mathbf{1}_{[a,b]}(\xi) = 1$ if $a \le \xi \le b$ and it is zero otherwise). The Shannon sampling process consists of an ideal low-pass pre-filtering and ideal sampler which

gives the discrete-time value $u[n] = x(nT)$ (if the support of $\hat{x}$ is included in $[-\pi/T, \pi/T]$). In reconstruction part we have $\tilde{\varphi}(t) = \text{sinc}(t/T)$, thus the Fourier transform is $\widehat{\tilde{\varphi}}(\xi) = T\mathbf{1}_{[\frac{-\pi}{T}, \frac{\pi}{T}]}(\xi)$. In fact the reconstruction process performs interpolation by sinc function.

From equations (4.9) and (4.13) it is not immediate that the output y is WSS for WSS input and that the sampling-reconstruction system is LSI. On the other hand if we examine equation (4.18), we can readily see that $\|H\| = \|G_c\|$, therefore $\text{SVM}(H) = 0$. It means that the Shannon's sampling-reconstruction process does not introduce shift-variance (i.e., it is LSI). Consequently $\text{ESV}(H, x) = \text{NSt}(Hx) = 0$ for each x.

4.1.2 B-spline Sampling

Now we consider the case where φ is taken to be B-spline of various order n [17]. Recall that $\beta^0(t) = \mathbf{1}_{[\frac{-T}{2}, \frac{T}{2}]}(t)$ (a box) and $\beta^n(t) = [\beta^0 * \beta^{n-1}](t)$. Note that B_0 is the simplest and shortest function that gives a Riesz basis [17]. B-splines of order $0 - 3$ with $T = 1$ are plotted in Figure 4.2.

It seems when n becomes larger the $B^n(t)$ looks more like the Gaussian kernel. To see that let $\{Z_k\}_{k \in \mathbb{N}}$ be independent identically distributed (iid) random variables whose probability density function (pdf) is $B^0(z)/T$. The mean of Z_k's is zero and their variance is $T^2/12$. The pdf of random variable $Z = \sum_{k=1}^{n} Z_k$ is $B^n(z)/T^n$. When n becomes large enough, by central limit theorem [10], Z tends to the Gaussian random variable with zero mean and variance of $nT^2/12$, thus we have

$$\lim_{n \to \infty} \frac{B^n(t)}{T^n} = \frac{\sqrt{12}}{\sqrt{2\pi n}T} \exp(-\frac{6t^2}{nT^2}) \tag{4.23}$$

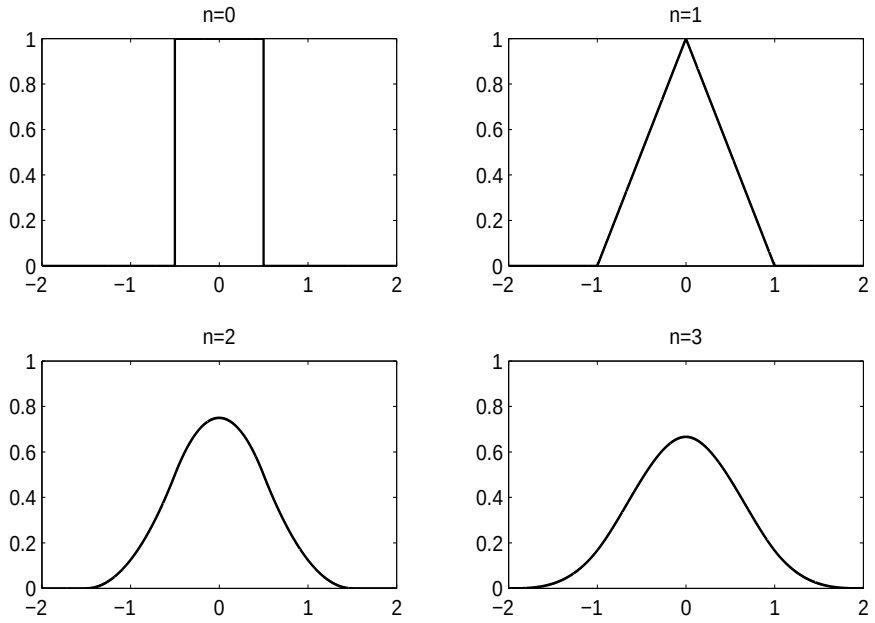

Figure 4.2: $B^n(t)$ with orders $n = 0,1,2,3$ and $T = 1$

and consequently

$$\lim_{n\to\infty} \widehat{B^n}(\xi) = T^n \exp(-\frac{n(T\xi)^2}{24}) \tag{4.24}$$

For $\varphi = \beta^0$, we have $\hat{\varphi}(\xi) = T\,\mathrm{sinc}(\xi/\omega_0)$ and $\{\varphi(\cdot - nT)\}_{n\in\mathbb{Z}}$ are orthogonal since they do not have overlap. By direct examination, the dual kernel is $\tilde{\varphi} = \frac{1}{T}\varphi$. Thus from equation (4.1), we have $\sum_{n\in\mathbb{Z}} |\hat{\varphi}(\xi + n\omega_0)|^2 = T^2$. Parseval's relation gives

$$\frac{1}{2\pi}\int_{-\infty}^{\infty} |\hat{\varphi}(\xi)|^2 \mathrm{d}\xi = \int_{-\infty}^{\infty} \left(\mathbf{1}_{[\frac{-T}{2},\frac{T}{2}]}(t)\right)^2 \mathrm{dt} = T$$

and

$$\frac{1}{2\pi}\int_{-\infty}^{\infty} |\hat{\varphi}(\xi)|^4 \,\mathrm{d}\xi = \int_{-\infty}^{\infty} \left([\mathbf{1}_{[\frac{-T}{2},\frac{T}{2}]} * \mathbf{1}_{[\frac{-T}{2},\frac{T}{2}]}](t)\right)^2 \mathrm{dt} = \frac{2}{3}T^3$$

Consequently $\mathrm{SVM}(H) = 1/\sqrt{3} = 0.5774 > 0.5$. This result indicates that H is quite shift-variant and $\mathrm{ESV}(H,x) = \mathrm{NSt}(Hx) = \mathrm{SVM}(H) = 0.5774$. It shows that the

behavior of system when is excited by a white noise is quite shift-variant and the output has considerable amount of non-stationarity. Since the kernel $B^0(t)$ is scaled by T, it is not surprising that SVM(H) is not related to T. If we look at equation (4.24), when n becomes larger the energy of $\widehat{B^n}(\xi)$ is mostly located in $[-\pi/T, \pi/T]$. Therefore it is expected that for each input x, NSt(Hx), ESV(H,x), SVM(H) can become arbitrary small if n is large enough.

When $n > 0$ or x is AR(1) random process, direct calculation of SVM, ESV, NSt is not easy. Thus we find them numerically. Since we have $\widehat{B^n}(\xi) = (T\text{sinc}(\xi/\omega_0))^n$ and the sinc function has very poor decay rate, in our numerical calculation we consider 500 summands for $|\hat{\varphi}(\xi + k\omega_0)|^2$ and also we consider the integration duration in $[-500, 500]$. The results for various order n are given in Table 4.1[2] .

We see that for $n = 0$, we have the worst shift-variance and non-stationarity. When $n = 1$, there is a big improvement but the sampling-reconstruction process is still considerably shift-variant and the output has considerable amount of non-stationarity. Not much improves for $n = 5, ..., 10$. When $n \geq 100$, the SVM, ESV, NSt are all less than 5%, we thus can say the sampling-reconstruction process is nearly shift-invariant and the output is nearly WSS. To make more sense of these results, we consider a particular example, $x_1(t) = \mathbf{1}_{[-1/2, 1/2]}(t)$ as input and the responses to the shifted versions of $x_1(t)$ in Figure 4.3 and Figure 4.4. The corresponding outputs are given in blue ($t_0 = 0$), green ($t_0 = 0.2$), magnolia ($t_0 = 0.4$), red ($t_0 = 0.5$), yellow ($t_0 = 0.6$), black ($t_0 = 0.8$) and in blue ($t_0 = 1$) respectively (the left column is the view from top for the right column). For $n = 0, 1$, we see the worst shift-variance. For $n = 2$, it seems that they look like each other but still there is big difference between them.

[2]The SVM is identical to ESV and NSt when the input x is white noise.

Table 4.1: SVM, ESV, NSt for Sampling-Reconstruction Process B-Spline of Various Order n with $T = 1$

Order n	SVM(H)(%) $S_x(\xi) = 1$	ESV(H,x) (%) $S_x(\xi) = \frac{1}{\xi^2+(0.9\pi)^2}$	NSt(Hx) (%) $S_x(\xi) = \frac{1}{\xi^2+(0.9\pi)^2}$
0	57.74	43.84	43.57
1	35.47	27.59	24.02
2	28.64	22.26	18.38
3	24.85	19.25	15.51
4	22.27	17.22	13.67
5	20.35	15.72	12.36
⋮	⋮	⋮	⋮
10	15.06	11.61	8.93
⋮	⋮	⋮	⋮
100	4.97	3.83	2.88
⋮	⋮	⋮	⋮
∞	0	0	0

When $n = 5$ or 10, the differences between shifted outputs become less, but we can still see the differences. For $n \geq 100$, we can hardly observe any difference between the shifted outputs and we can say the sampling-reconstruction process is nearly shift-invariant. The SVM and the results in this particular example are compatible.

4.2 Discrete Wavelet Transforms

Now consider the discrete wavelet analysis-synthesis as sampling-reconstruction process. Let $\psi(t)$ be a wavelet function and $\tilde{\psi}(t)$ be its biorthogonal function. Similar to [21], for two scalars $a, b > 0$ we can define

$$\psi_{m,n} = a^{-m/2}\psi(a^{-m}t - bn), \quad m,n \in \mathbb{Z} \tag{4.25}$$

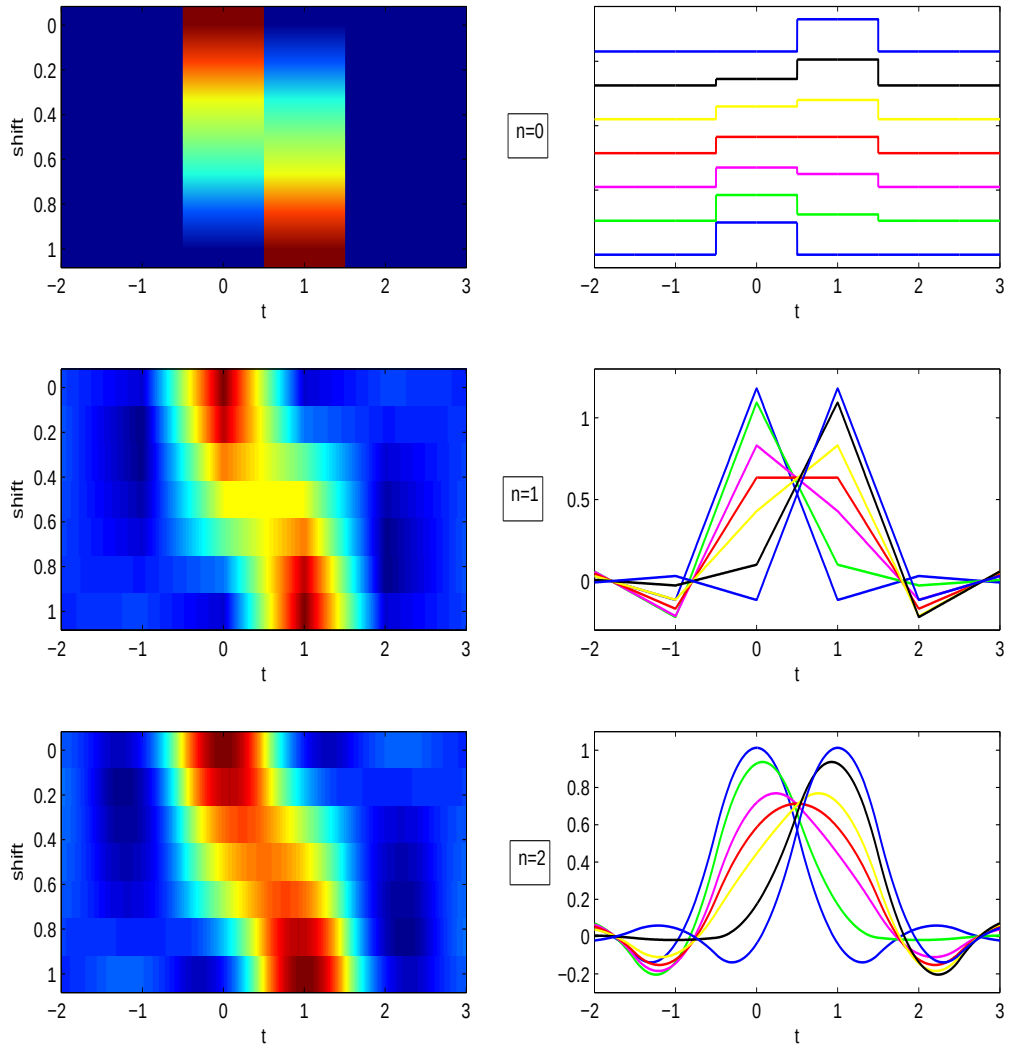

Figure 4.3: The outputs of B-spline sampling-reconstruction process with orders $n = 0, 1, 2$ and $T = 1$ for the shifted particular inputs

Therefore the DWT is defined as

$$x(t) \mapsto \{\langle x, \tilde{\psi}_{m,n} \rangle\}_{m,n \in \mathbb{Z}} \tag{4.26}$$

and the synthesis is

$$y_m(t) = \sum_{n \in \mathbb{Z}} \langle x, \tilde{\psi}_{m,n} \rangle \psi(t)_{m,n} \tag{4.27}$$

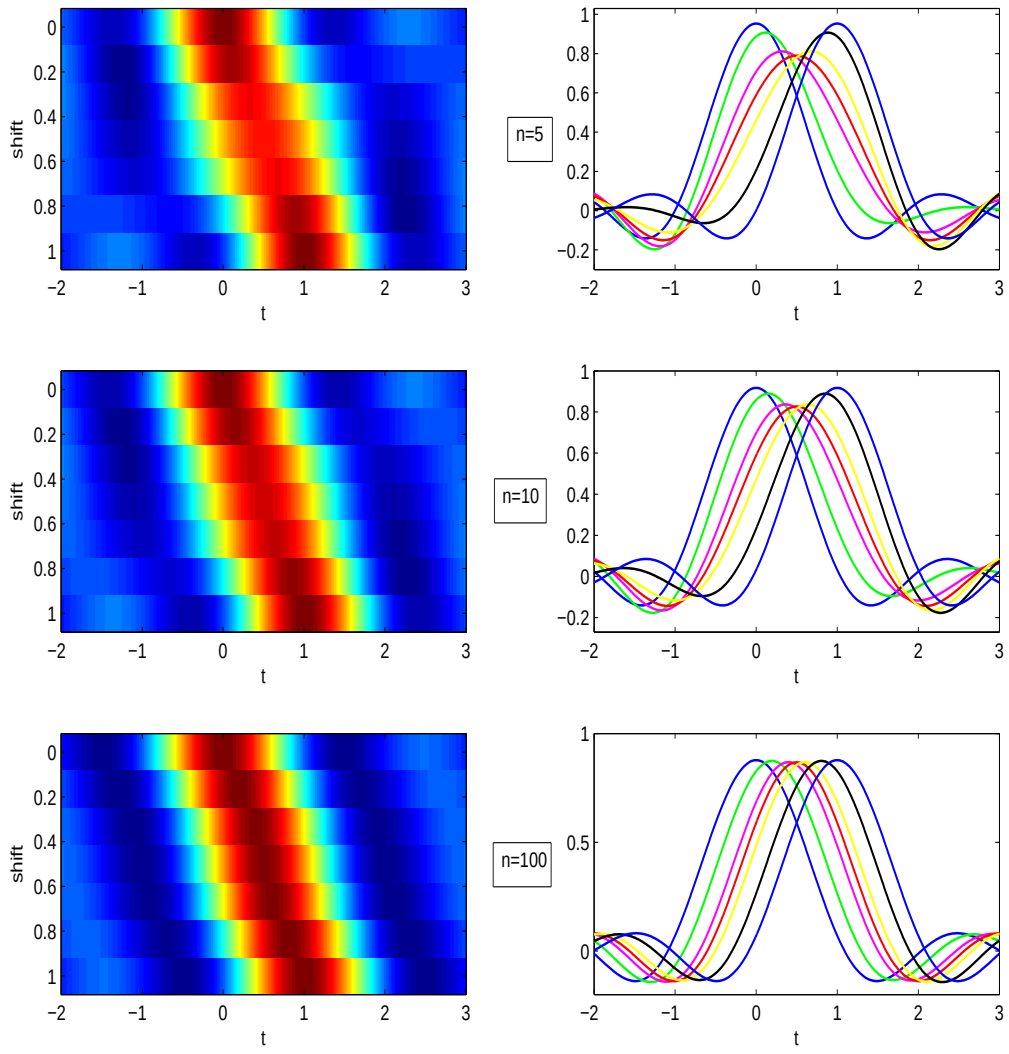

Figure 4.4: The outputs of B-spline sampling-reconstruction process with orders $n = 5$, 10, 100 and $T = 1$ for the shifted particular inputs

For each m, the DWT is a sampling process and synthesis is reconstruction process with $\varphi = \psi_{m,0}$ and $T = a^m b$. Thus we can apply the preceding results to the DWTs.

We obtain the SVM, ESV and NSt of six wavelets, three of them are real and the three of them are complex. The wavelets and their Fourier transforms are listed in Table 4.2 and the magnitudes are plotted in Figure 4.5. For simplicity we assume $m = 0$, $b = 1$, thus $T = b = 1$. Again we use numerical methods to obtain SVM, ESV and NSt. But since the decay rate of these six wavelets is fast, we consider 10 terms in summand

Table 4.2: Six Wavelets, First Three Real and Last Three Complex

Wavelet	$\hat{\psi}(\xi)$
Shannon	$\begin{cases} e^{-j\xi/2}, & \lvert\xi\rvert \in [\pi, 2\pi) \\ 0 & \text{otherwise} \end{cases}$
Mexican hat	$-\sqrt{\frac{8}{3}}\pi^{1/4}\xi^2 e^{-\xi^2/2}$
Meyer	$\begin{cases} (2\pi)^{-1/2}e^{j\xi/2}\sin\left(\frac{\pi}{2}v(\frac{3}{2\pi}\lvert\xi\rvert-1)\right), & \lvert\xi\rvert \in [2\pi/3, 4\pi/3) \\ (2\pi)^{-1/2}e^{j\xi/2}\cos\left(\frac{\pi}{2}v(\frac{3}{4\pi}\lvert\xi\rvert-1)\right), & \lvert\xi\rvert \in [4\pi/3, 8\pi/3) \\ 0 & \text{otherwise} \end{cases}$ where $v(s) = s^4(35-84s+70s^2-20s^3)$, $s \in [0,1)$
Complex Shannon	$\begin{cases} e^{-j\xi/2}, & \lvert\xi\rvert \in [\pi, 3\pi) \\ 0 & \text{otherwise} \end{cases}$
Complex Morlet	$\pi^{-1/4}\left(e^{-(\xi-5)^2} - e^{-(\xi+25)/2}\right)$
Hermitian hat	$\frac{2}{\sqrt{5}}\pi^{-1/4}\xi(1+\xi)e^{-\xi^2/2}$

and also for integration duration, the interval $[-3\pi, 3\pi]$ is adequate. The results are given in Table 4.3. We can realize that generally complex wavelets have less SVM, ESV, NSt. It seems Complex Morlet is near shift-invariant for deterministic input. For complex Morlet, unlike the other wavelets, when the input is AR(1), the ESV of the wavelet and the non-stationary of its output is more than its SVM. The reason is the particular choice of α in AR(1).

To make more sense, we take a particular example where the input is assumed to be $x_2(t) = \mathbf{1}_{[0,1/2]}(t) - \mathbf{1}_{[-1/2,0]}(t)$. The plot of $x(t)$ is given in Figure 4.6. (Note that

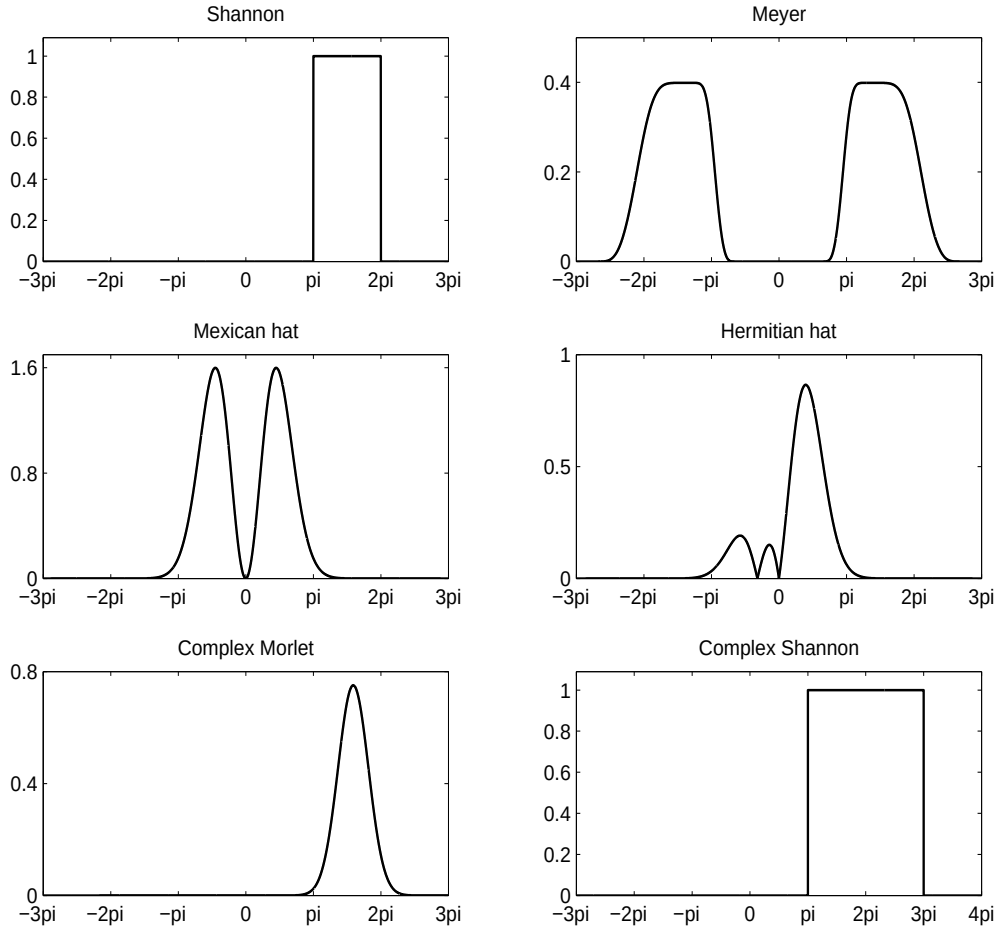

Figure 4.5: Plots of $|\hat{\psi}(\xi)|$ for Six Wavelets

Table 4.3: SVM, ESV, NSt for Six Wavelets with $T = 1$

	SVM(H)(%)	ESV(H,x) (%)	NSt(Hx) (%)
Wavelet	$S_x(\xi) = 1$	$S_x(\xi) = \frac{1}{\xi^2+(0.9\pi)^2}$	
Shannon	0	0	0
Mexican hat	17.86	13.37	10.72
Meyer	35.83	34.79	35.64
Complex Shannon	0	0	0
Complex Morlet	11.20	13.09	14.45
Hermitian hat	18.02	13.92	10.86

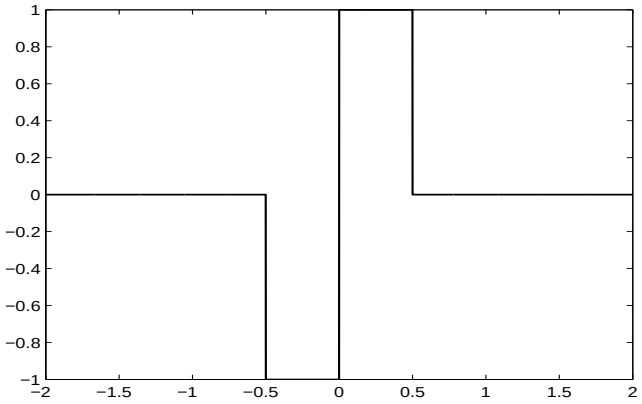

Figure 4.6: The particular input signal for wavelets

wavelet transform-synthesis is relevant for input signals with high frequency components, unlike the B-spline sampling-reconstruction processes we consider different input for wavelets which work better for inputs with low frequency components) We shift the input $x_2(t)$ and we show the corresponding outputs in blue ($t_0 = 0$), green ($t_0 = 0.2$), magnolia ($t_0 = 0.4$), red ($t_0 = 0.5$), yellow ($t_0 = 0.6$), black ($t_0 = 0.8$) and in blue ($t_0 = 1$) respectively. The results are illustrated in Figure 4.7 where the left column is the view from top for the right column. As expected, the complex wavelet transforms are less shift-variant. Complex Morlet seems to be nearly shift-invariant. On the other hand the shift-variance for Meyer is high, whereas those for complex Hermitian and Mexican hat are similar.

In another particular example, we obtain the autocorrelation functions of the outputs of four wavelet sampling-reconstruction processes when the input is white noise. We obtain the autocorrelation of outputs in various time that are specified by in blue ($t = 0$), green ($t = 0.2$), magnolia ($t = 0.4$), red ($t = 0.5$), yellow ($t = 0.6$) and in black ($t = 0.8$) respectively. The result are illustrated in Figure 4.8 where the left column is the view from top for the right column. Again as expected, the output for complex Molrlet is nearly WSS. The non-stationarity of the output for Mexican hat is approximately equal

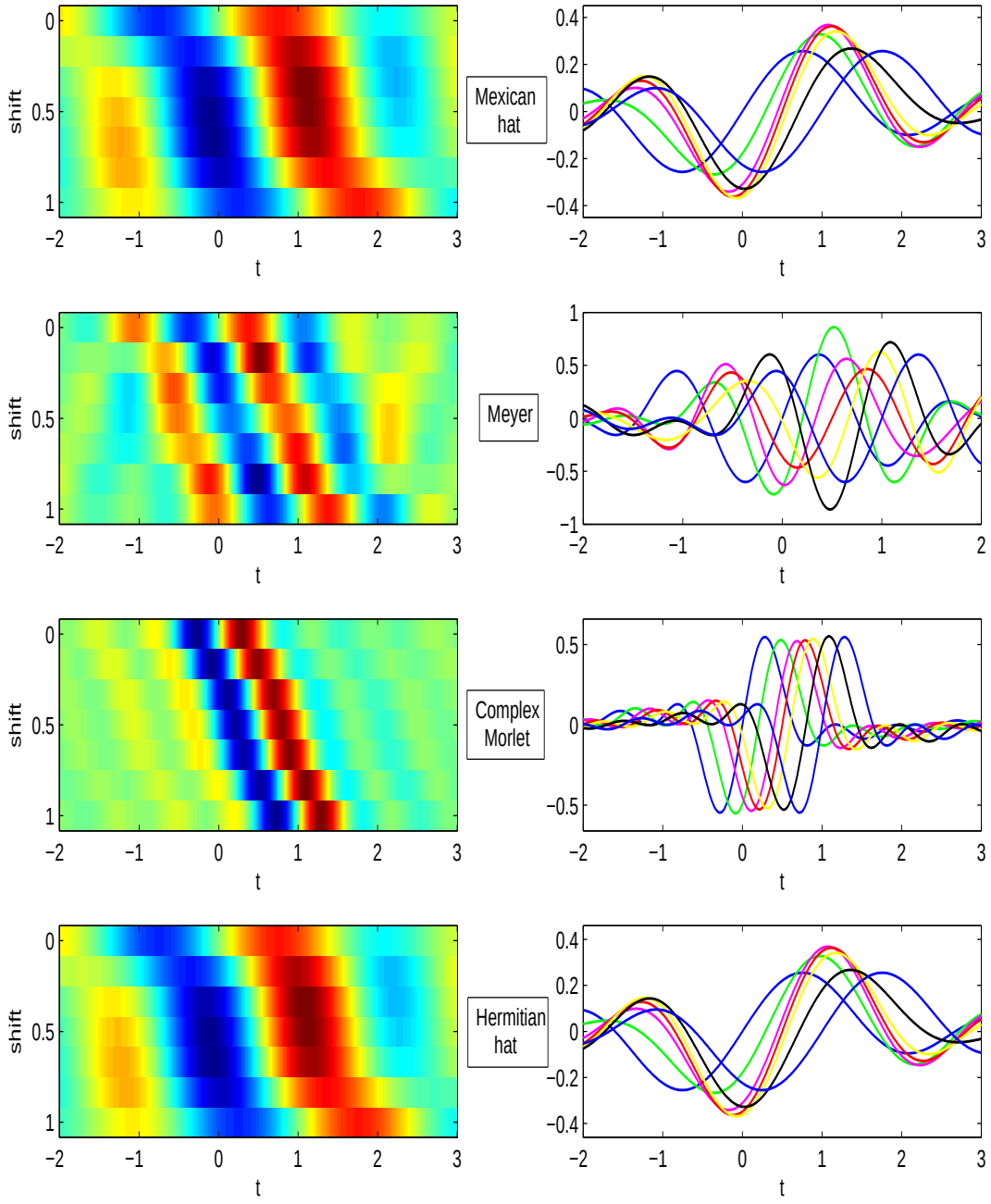

Figure 4.7: The outputs of four wavelets for the shifted particular inputs

to the non-stationarity of the output for complex Hermitian. the output of Meyer has the worst non-stationarity.

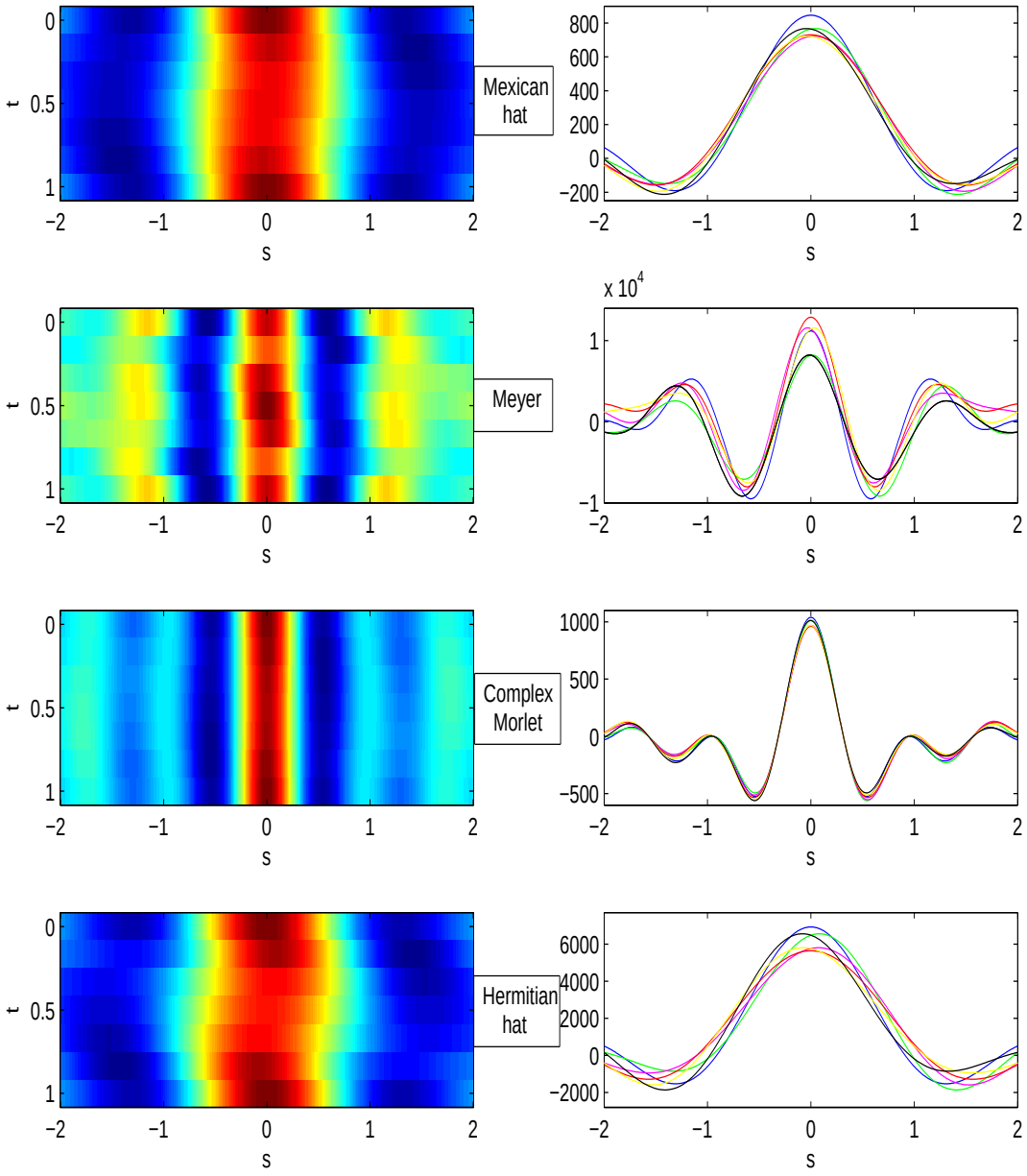

Figure 4.8: The autocorrelation of four wavelets with white noise input

4.3 Double Sideband Amplitude Modulation Systems and Signals

In this section we study the DSB-AM systems and signals. It is well-known that the input-output relation of the DSB-AM system [9] is

$$H : x(t) \mapsto y(t) = x(t)\cos(\omega_c t) \tag{4.28}$$

where the carrier frequency ω_c is constant. The impulse response is

$$h(t,s) = \delta(s)\cos(\omega_c t) \tag{4.29}$$

Note that we have $h(t+T_c,s) = h(t,s)$ where $T_c = 2\pi/\omega_c$. Thus, the DSB-AM system is T_c-LPSV. The Fourier series representation of $h(t,s)$ is

$$h(t,s) = \frac{1}{2}\delta(s)\left(e^{-j\omega_c t} + e^{j\omega_c t}\right) \tag{4.30}$$

Since there is delta function in $h(t,s)$, the norm and SVL of H is infinity. At first glance we can not compute the SVM, but we can overcome this difficulty by using the non-ideal impulse response. For $\varepsilon > 0$ define the system H_ε by its Greens's function as

$$\begin{aligned} k_\varepsilon(t,s) &= \frac{1}{2\varepsilon}[H\left(\mathbf{1}_{[-\varepsilon,\varepsilon]}(\cdot - s)\right)](t) \\ &= \frac{1}{2\varepsilon}\mathbf{1}_{[-\varepsilon,\varepsilon]}(t-s)\cos(\omega_c t) \end{aligned} \tag{4.31}$$

Obviously $k_\varepsilon(t,s)$ and $k(t,s)$ are related as

$$k(t,s) = \lim_{\varepsilon\to 0} k_\varepsilon(t,s) \tag{4.32}$$

Consequently the impulse response of H_ε is

$$\begin{aligned} h_\varepsilon(t,s) &= k_\varepsilon(t,t-s) \\ &= \frac{1}{4\varepsilon}\mathbf{1}_{[-\varepsilon,\varepsilon]}(s)\left(e^{-j\omega_c t} + e^{j\omega_c t}\right) \end{aligned} \tag{4.33}$$

Therefore we have

$$h(t,s) = \lim_{\varepsilon\to 0} h_\varepsilon(t,s) \tag{4.34}$$

and lousily

$$H = \lim_{\varepsilon \to 0} H_\varepsilon \tag{4.35}$$

The norm of H_ε is obtained as

$$\|H_\varepsilon\|^2 = \frac{1}{4\varepsilon} \tag{4.36}$$

Since the DC part of $h_\varepsilon(t,s)$ as a function of t is zero (i.e., H_ε is orthogonal to the subspace $\mathcal{B}_0$), therefore the distance to the nearest LSI system is

$$d(H_\varepsilon, \mathcal{B}_0) = \|H_\varepsilon\| \tag{4.37}$$

and consequently we have

$$\mathrm{SVM}(H) = \lim_{\varepsilon \to 0} \frac{d(H_\varepsilon, \mathcal{B}_0)}{\|H_\varepsilon\|} = 1 \tag{4.38}$$

This result indicates that the average of norm of $H_\varepsilon \tau_{t_0} - \tau_{t_0} H_\varepsilon$, which generates the difference between shifted output and response to the shifted input (commutator), reaches the upper-bound ($\sqrt{2}\|H_\varepsilon\|$). Similarly we can show that

$$\mathrm{ESV}(H,x) = 1 \ \text{ for each } \ x \tag{4.39}$$

This result indicates that the average of expected value of $|(H_\varepsilon \tau_{t_0} - \tau_{t_0} H_\varepsilon)x|^2$ reaches its upper-bound (the average of expected value of $2|H_\varepsilon x|^2$).

The autocorrelation function of DSB-AM signal y under WSS input x is

$$\begin{aligned} r_y(t,s) &= \frac{1}{4}\mathcal{E}\{x(t)\left(e^{-j\omega_c t}+e^{j\omega_c t}\right)\overline{x(t-s)}\left(e^{-j\omega_c(t-s)}+e^{j\omega_c(t-s)}\right)\} \\ &= \frac{1}{4}r_x(s)\left(e^{-j\omega_c(2t-s)t}+2\cos\omega_c s+e^{j\omega_c(2t-s)t}\right) \end{aligned} \tag{4.40}$$

This shows that y is a $T_c/2-$WSCS random process. In the Fourier domain, we have

$$R_y(t,\xi)=\frac{1}{4}\left(R_x(\xi-\omega_c)e^{-j2\omega_c t}+R_x(\xi-\omega_c)+R_x(\xi+\omega_c)+R_x(\xi+\omega_c)e^{j2\omega_c t}\right) \tag{4.41}$$

When the input x is a white noise, the energy of $r_x(s)=\delta(s)$ is unbounded. Thus we consider the autocorrelation function

$$r_\varepsilon(s)=\frac{1}{\pi\varepsilon}\mathrm{sinc}(\frac{s}{\pi\varepsilon}) \tag{4.42}$$

In this situation

$$R_\varepsilon(\xi)=\mathbf{1}_{[-\frac{1}{\varepsilon},\frac{1}{\varepsilon}]}(\xi) \tag{4.43}$$

and

$$\lim_{\varepsilon\to 0} r_\varepsilon(s)=r_x(s) \tag{4.44}$$

Therefore

$$\begin{aligned} \mathrm{NSt}^2(y) &= 1-\lim_{\varepsilon\to 0}\frac{|R_\varepsilon(\xi-\omega_c)+R_\varepsilon(\xi+\omega_c)|^2}{|R_\varepsilon(\xi-\omega_c)|^2+|R_\varepsilon(\xi-\omega_c)+R_\varepsilon(\xi+\omega_c)|^2+|R_\varepsilon(\xi+\omega_c)|^2} \\ &= \frac{1}{3} \end{aligned} \tag{4.45}$$

It means $\mathrm{NSt}(y)=57.74\,\%$, therefore the output is quite non-stationary in wide-sense.

Chapter 5

CONCLUSIONS AND FUTURE WORK

We reported in this thesis our latest study on shift-variance and non-stationarity analysis of LPSV systems and WSCS random processes. We extended recent similar results to systems with continuous-time input and output. The extension enables us to define and compute the following:

- The SVL and SVM for LPSV systems and the ESV for LPSV systems when the input is WSS random process.
- The non-stationarity of a WSCS random process.

We then studied generalized sampling-reconstruction processes, DWTs and DSB-AM systems and signals. B-splines sampling-reconstruction with orders greater than 100 are near shit-invariant and generate nearly WSS random processes for WSS random inputs. It seems complex analysis-synthesis wavelet (especially complex Morlet) transforms generally have good shift-invariant property. The DSB-AM systems are fully (100%) shift-variant under both deterministic and stochastic inputs. The DSB-AM white noise has considerable amount of non-stationarity (57.74%).

As future work we hope to find the relation between the error of linear optimal filtering (Wiener filter) under jointly WSCS random processes and the NSt or the ESV of the linear system which is generating the WSCS signals.

REFERENCES

[1] T. Aach,"Comparative Analysis of Shift Variance and Cyclostationarity in Multirate Filter Banks, *IEEE Trans. Circuits Syst. I: Reg. Papers.*, vol. 54, pp. 1077-1087, May 2007.

[2] T. Aach and H. Führ, "On Bounds of Shift Variance in Two-Channel Mutirate Filter Banks," *IEEE Trans. Signal Process.*, vol. 57, pp. 4292–4303, Nov. 2009.

[3] T. Aach and H. Fuhr, "Shift variance, Cyclostationarity and Expected Shift Variance in Multirate LPSV Systems," *Proc. 2011 IEEE Statis. Signal Process. Workshop.*, pp. 785-788, Nice, France, Jun. 2011

[4] T. Aach and H. Führ, "Shift Variance Measures for Multirate LPSV Filter Banks with Random Input Signals," *IEEE Trans. Signal Process.*, vol. 60, pp. 5124–5134, Oct. 2012.

[5] S. Akkarakaran and P. P. Vaidyanathan, "Bifrequency and Bispectrum Maps: A New Look at Multirate Systems with Stochastic Inputs," *IEEE Trans. Signal Process.*, vol. 48, no. 3, pp. 723–736, Mar. 2000.

[6] S. A. Benno and J. M. F. Moura, "Scaling Functions Robust to Translations," *IEEE Trans. Signal Process.*, vol. 46, no. 12, pp. 3269–3281, Dec. 1998.

[7] T. Chen and L. Qiu, "Linear Periodically Time-Varying Discrete-Time Systems: Aliasing and LTI Approximation," *Syst. and Control Lett.*, vol. 30, pp. 225–235, 1997.

[8] L. E. Franks, *Signal Theory.*, Revised, Pearson Prentice Hall, Pearson Education, 1981.

[9] W. A. Gardner, A. Napolitano and L. Paura, “Cyclostationarity: Half A Century of Research,” *Signal Process.*, vol. 86, pp. 639–697, 2006.

[10] A. Leon-Garcia, *Probability, Statistics, and Random Processes for Electrical Engineering.*, Pearson Prentice Hall, Pearson Education, Inc, 2008.

[11] S. Mallat, *A Wavelet Tour of Signal Processing: The Sparse Way.*, Amsterdam: Academic Press, 2009.

[12] A. V. Oppenheim, R. W. Schafer and with J. R. Buck, *Discrete-Time Signal Processing.*, New Jersey: Prentice-Hall, 1999.

[13] A. Papoulis, *Probability, Random Variables, and Stochastic Processes.*, New York: McGraw-Hill, 1965.

[14] B. Sadeghi and R. Yu, “Shift-Variance and Cyclostationarity of Linear Periodically Shift-Variant Systems,” *10’th Int. Conf. On Sampling Process Theory and App.*, Bremen, Germany, July 2013.

[15] V. P. Sathe and P. P. Vaidyanathan, “Effects of multirate systems on the statistical properties of random signals,”*IEEE Trans. Signal Processing.*, vol. 41, pp. 131-146, Jan. 1993.

[16] G. Strang and T. Nguyen, *Wavelets and Filterbanks.*, Wellesley, MA: Wellesley-Cambridge Press, 1997.

[17] M. Unser, “Sampling — 50 Years After Shannon,” *Proc. IEEE.*, vol. 88, pp. 569–587, Apr. 2000.

[18] M. Unser and A. Aldroubi, “A General Sampling Theory for Nonideal Acquisition Devices,” *IEEE Trans. Signal Process.*, vol. 42, pp. 2915–2925, Nov. 1994.

[19] R. Yu, “A New Shift-Invariance of Discrete-Time Systems and its Application to Discrete Wavelet Transform Analysis,” *IEEE Trans. Signal Process.*, vol. 57, pp. 2527-2537, Jul. 2009.

[20] R. Yu, “Shift-Variance Measure of Multichannel Multirate Systems,” *IEEE Trans. Signal Process.*, vol. 59, pp. 6245–6250, Dec. 2011.

[21] R. Yu, “Shift-variance Analysis of Generalized Sampling Process ,” *IEEE Trans. Signal Process.*, vol. 60, pp. 2840–2850, Jun. 2012.

[22] G. D. Zivanovic and W. A. Gardner, “Degrees of Cyclostationarity and Their Application to Signal Detection and Estimation,” *Signal Process.*, vol. 22, pp. 287–297, 1991.

APPENDICES

Appendix A: Proof of Theorem 1

From (2.19), $\kappa_{t_0}(t,s) = h(t,s-t_0) - h(t-t_0,s-t_0)$, therefore

$$\|\mathcal{K}_{t_0}\|^2 = \frac{1}{T}\int_{-T/2}^{T/2}\int_{\infty}^{\infty} |h(t,s-t_0) - h(t-t_0,s-t_0)|^2 \,\mathrm{ds}\,\mathrm{dt}$$

Invoking Parseval's relation in Fourier series gives

$$\begin{aligned} \|\mathcal{K}_{t_0}\|^2 &= \sum_{k\in\mathbb{Z}} \int_{-\infty}^{\infty} |h_k(s-t_0) - h_k(s-t_0)e^{-jk\omega_0 t_0}|^2 \,\mathrm{ds} \quad \text{(by change } u = s-t_0\text{)} \\ &= \sum_{k\in\mathbb{Z}} \int_{-\infty}^{\infty} |h_k(u) - h_k(u)e^{-jk\omega_0 t_0}|^2 \,\mathrm{du} \end{aligned}$$

The above equation shows that $\|\mathcal{K}_{t_0}\|$ is $T-$periodic in t_0. Again invoking Parseval's relation for Fourier series results

$$\begin{aligned} \mathrm{SVL}^2(H) &= \frac{1}{T}\int_{-T/2}^{T/2} \|\mathcal{K}_{t_0}\|^2 \,\mathrm{dt}_0 \\ &= 2\sum_{k\neq 0} \int_{\infty}^{\infty} |h_k(s)|^2 \,\mathrm{ds} = 2\,d^2(H,\mathcal{B}_0) \end{aligned}$$

Appendix B: Derivation of Equations (3.5) and (3.6)

$$\begin{aligned} r(t,s) &= \mathcal{E}\{y(t)\,\overline{y(t-s)}\} \\ &= \mathcal{E}\int_{-\infty}^{\infty}\int_{-\infty}^{\infty} h(t,s_1)\,x(t-s_1)\,\overline{h(t-s,s_2)}\,\overline{x(t-s-s_2)}\,\mathrm{ds}_1\,\mathrm{ds}_2 \end{aligned}$$

Since x is WSS, thus

$$r(t,s) = \int_{-\infty}^{\infty}\int_{-\infty}^{\infty} h(t,s_1)\,\overline{h(t-s,s_2)}\,r_x(s+s_2-s_1)\,\mathrm{ds}_1\,\mathrm{ds}_2$$

This equation shows that $r(t,s)$ is $T-$periodic in t (i.e., the output of H is $T-$WSCS).

Representing $h(t,s)$ in the Fourier series, we get

$$r(t,s) = \int_{-\infty}^{\infty}\int_{-\infty}^{\infty} A(s_1)\,B(s_2)\,r_x(s+s_2-s_1)\,\mathrm{d}s_1\,\mathrm{d}s_2$$

where

$$A(s_1) = \sum_{k\in\mathbb{Z}} h_{k_1}(s_1)e^{jk\omega_0 t} \text{ and } B(s_2) = \sum_{k\in\mathbb{Z}} \overline{h_{k_2}(s_2)}e^{-jk\omega_0(t-s)}$$

After taking Fourier transform as a function of s, we get

$$\begin{aligned} S(t,\xi) &= \int_{-\infty}^{\infty}\int_{-\infty}^{\infty} A(s_1)\,C(s_1,s_2)\,\mathrm{d}s_1\,\mathrm{d}s_2 \\ &= \sum_{k_1\in\mathbb{Z}}\sum_{k_2\in\mathbb{Z}} \hat{h}_{k_1}(\xi-k\omega_0)\overline{\hat{h}_{k_2}(\xi-k_2\omega_0)}S_x(\xi-k_2\omega_0)e^{j(k_1-k_2)\omega_0 t} \end{aligned}$$

where

$$C(s_1,s_2) = \sum_{k\in\mathbb{Z}} \overline{h_{k_2}(s_2)}S_x(\xi-k_2\omega_0)e^{-j(\xi-k\omega_0)(s_1-s_2)}$$

By change of variable $k = k_1 - k_2$ and $l = k_2$, we have

$$S(t,\xi) = \sum_{k\in} \left(\sum_{l\in\mathbb{Z}} \hat{h}_{(k+l)}(\xi-l\omega_0)\,\overline{\hat{h}_l(\xi-l\omega_0)}\,S_x(\xi-l\omega_0) \right) e^{jk\omega_0 t}$$

Thus the coefficients of $S(t,\xi)$ are

$$S_k(\xi) = \sum_{l\in\mathbb{Z}} \hat{h}_{(k+l)}(\xi-l\omega_0)\,\overline{\hat{h}_l(\xi-l\omega_0)}S_x(\xi-l\omega_0)$$

Multiplication in the frequency domain corresponds to convolution in the time domain.

Then

$$r_k(s) = \sum_{l\in\mathbb{Z}} [h_{(k+l)} * r_x * \tilde{h}_l](s)\, e^{jl\omega_0 s}$$

Appendix C: Derivation of Equations (3.13)

$$|Hx|^2 = \int_{-\infty}^{\infty}\int_{-\infty}^{\infty} h(t,s_1)\,\overline{h(t,s_2)}\,x(t-s_1)\,\overline{x(t-s_2)}\,\mathrm{d}s_1\,\mathrm{d}s_2$$

Since x is WSS, therefore

$$\mathcal{E}\{|[Hx](t)|^2\} = \int_{-\infty}^{\infty}\int_{-\infty}^{\infty} h(t,s_1)\,\overline{h(t,s_2)}\,r_x(s_2-s_1)\,\mathrm{d}s_1\,\mathrm{d}s_2$$

Using Parseval's relation we get

$$\begin{aligned}\mathcal{E}\{|[Hx](t)|^2\} &= \frac{1}{2\pi}\int_{-\infty}^{\infty}\int_{-\infty}^{\infty} h(t,s_1)\,\overline{\hat{h}(t,\xi)}\,S_x(\xi)e^{-js_1\xi}\,\mathrm{d}s_1\,\mathrm{d}\xi \\ &= \frac{1}{2\pi}\int_{-\infty}^{\infty} |\hat{h}(t,\xi)|^2\,S_x(\xi)\,\mathrm{d}\xi\end{aligned}$$

Similarly

$$\mathcal{E}\{|d_{t_0}(t)|^2\} = \mathcal{E}\{|[\mathcal{K}_{t_0}x](t)|^2\} = \frac{1}{2\pi}\int_{\infty}^{\infty} |\hat{\kappa}_{t_0}(t,\xi)|^2 S_x(\xi)\,\mathrm{d}\xi$$

Since $\hat{\kappa}_{t_0}(t,\xi)$ as a function of t is $T-$periodic, we can represent it in Fourier series.

From (2.19), the Fourier series coefficients of $\hat{\kappa}_{t_0}(t,\xi)$ are

$$\hat{h}_k(\xi)\,(1-e^{-jk\omega_0 t_0})\,e^{-j\xi t_0}$$

Using Parseval's relation, we see that

$$\frac{1}{T}\int_{-T/2}^{T/2}\mathcal{E}\{|d_{t_0}(t)|^2\}\,\mathrm{d}t=\frac{1}{2\pi}\sum_{k\in\mathbb{Z}}\int_{\infty}^{\infty}|\hat{h}_k(\xi)\,(1-e^{-jk\omega_0 t_0})\,S_x(\xi)|^2\,\mathrm{d}\xi$$

The above statement is $T-$periodic in t_0. Again invoking Parseval's relation for Fourier series gives

$$\frac{1}{T^2}\int_{-T/2}^{T/2}\int_{-T/2}^{T/2}\mathcal{E}\{|d_{t_0}(t)\}|^2\,\mathrm{d}t\,\mathrm{d}t_0=\frac{1}{\pi}\sum_{k\neq 0}\int_{-\infty}^{\infty}|\hat{h}_k(\xi)|^2\,S_x(\xi)\,\mathrm{d}\xi$$

and

$$\frac{2}{T}\int_{-T/2}^{T/2}\mathcal{E}\{|[Hx](t)|^2\}\,\mathrm{d}t=\frac{1}{\pi}\sum_{k\in\mathbb{Z}}\int_{-\infty}^{\infty}|\hat{h}_k(\xi)|^2\,S_x(\xi)\,\mathrm{d}\xi$$

Appendix D: Derivation of Equation (4.10)

From (4.9) we have

$$r_y(t,s)=\sum_{n_1\in\mathbb{Z}}\sum_{n_2\in\mathbb{Z}}\varphi(t-n_1T)\,\overline{\varphi(t-s-n_2T)}\,r_u[n_1-n_2]$$

Taking Fourier transform of $r_y(t,s)$ as a function of s yields

$$\begin{aligned}S_y(t,\xi) &= \overline{\hat{\varphi}(\xi)}\,e^{-j\xi t}\sum_{n_1\in\mathbb{Z}}\sum_{n_2\in\mathbb{Z}}\varphi(t-n_1T)\,r_u(n_1-n_2)\,e^{j\xi n_2T}\\ &= \overline{\hat{\varphi}(\xi)}\,e^{-j\xi t}\,S_u(e^{j\xi T})\sum_{n_1\in\mathbb{Z}}\varphi(t-n_1T)\,e^{j\xi n_1T}\end{aligned}$$

The Fourier series coefficients of $S_y(t,\xi)$ are

$$(S_y)_k(\xi)=\frac{1}{T}\overline{\hat{\varphi}(\xi)}\,S_u(e^{j\xi T})\sum_{n_1\in\mathbb{Z}}\int_{-T/2}^{T/2}e^{j\xi n_1T}\,\varphi(t-n_1T)\,e^{-j\xi t}\,e^{-jk\omega_0 t}\,\mathrm{d}t$$

By change of variable $(t + n_1 T) \to t$, we get

$$\begin{aligned}
(S_y)_k(\xi) &= \frac{1}{T}\overline{\hat{\varphi}(\xi)}\, S_u(e^{j\xi T}) \sum_{n_1 \in \mathbb{Z}} \int_{-T/2-n_1 T}^{T/2-n_1 T} \varphi(t)\, e^{-j\xi t}\, e^{-jk\omega_0 t}\, \mathrm{dt} \\
&= \frac{1}{T}\overline{\hat{\varphi}(\xi)}\, S_u(e^{j\xi T}) \int_{-\infty}^{\infty} \varphi(t)\, e^{-j(\xi + k\omega_0)t}\, \mathrm{dt} \\
&= \frac{1}{T}\overline{\hat{\varphi}(\xi)}\, S_u(e^{j\xi T})\, \hat{\varphi}(\xi + k\omega_0)
\end{aligned}$$